

$Ln_2Sr_2PtO_{7+\delta}$ ($Ln = La, Pr, \text{ and } Nd$): Three new Pt-containing $[A'_2O_{1+\delta}][A_nB_{n-1}O_{3n}]$ -type hexagonal perovskites

Stefan G. Ebbinghaus^{a,*}, Chasanoglou Erztoument^a, Ivan Marozau^b

^aLehrstuhl für Festkörperchemie, Institut für Physik, Universität Augsburg, Universitätsstraße 1, D-86159 Augsburg, Germany

^bPaul Scherrer Institut, CH-5232 Villigen PSI, Switzerland

Received 20 July 2007; received in revised form 1 October 2007; accepted 1 October 2007

Available online 7 October 2007

Abstract

Polycrystalline samples of $Ln_2Sr_2PtO_{7+\delta}$ ($Ln = La, Pr, Nd$) were prepared by conventional solid state synthesis. The three compounds are new examples for $n = 2$ members of the $[A'_2O_{1+\delta}][A_nB_{n-1}O_{3n}]$ family of hexagonal perovskites containing platinum as the B -type cation. XRD Rietveld refinements show the platinates to crystallize in space group $R\bar{3}$ and, in the case of Pr and Nd, revealed a complete ordering of Ln/Sr on the two distinct A -type positions, while for La a partial disorder was observed. By XANES investigations at the Pt- L_{III} threshold the oxidation state +4 for platinum was found. Thermogravimetry revealed a small oxygen excess for $Ln = La$ and Pr ($\delta = 0.13$ and 0.07), pointing to the presence of peroxide ions as already observed for isostructural Ru- and Ir-based compounds. UV-Vis measurements were done for the yellow lanthanum and the green neodymium compound. They revealed two optical band gaps of 2.52 and 3.05 eV, respectively. Magnetic measurements showed $La_2Sr_2PtO_{7+\delta}$ to be diamagnetic as expected for Pt^{4+} with low-spin (t_{2g}^6) configuration. For $Ln = Pr$ and Nd the observed strong paramagnetism can be explained solely by the magnetic moments of the rare earths.

© 2007 Elsevier Inc. All rights reserved.

Keywords: Hexagonal perovskites; Platinates; XRD Rietveld refinements; Thermogravimetry; Magnetic properties; Optical spectroscopy

1. Introduction

The family of hexagonal perovskites can be described by a hexagonal close packing of AO_3 -layers (stacking sequence *ababab*...) in which the B -cations occupy 1/4 of the octahedral sites. This arrangement results in chains of face-sharing BO_6 -octahedra. In the aristotype (the so-called 2H structure) these chains are in principle infinite. Many modified structures exist, in which the chains are interrupted by, for example, trigonal prisms. These structures can often be grouped in homologous series. One specific family of hexagonal perovskites possesses the general composition $[A'_2O_{1+\delta}][A_nB_{n-1}O_{3n}]$, where $n-1$ reflects the number of face-sharing BO_6 -octahedra. In these compounds, the BO_6 -chains are interrupted by $[A'_2O_{1+\delta}]$ -layers in which six trigonal prisms form large

hexagonal cavities. These cavities can be occupied by oxide ions (O^{2-}), or peroxide ions (O_2^{2-}). The few examples of this family of hexagonal perovskites reported so far contain the transition metals Mn, Nb, Ru, and Ir and belong to $n = 6, 3,$ and $2,$ respectively. The only $n = 6$ oxide known to date is $La_4Ba_{2.6}Ca_{1.4}(Mn_4Ca)O_{19}$ [1]. This oxide also includes structural features typical for the family of cubic perovskites, i.e. corner-sharing octahedra. Most compounds described in literature belong to the $n = 3$ structure: $La_2Ba_{0.8}Sr_{0.6}Ca_{1.6}Mn_2O_{10}$ [2], $Ba_5Nb_2O_9(O_2)$ [3], $Ba_5Ru_2O_{10}$ [4], $Ba_5Ru_2O_9(O_2)$ [5], and $Ba_{3.44}K_{1.56}Ir_2O_{10}$ [6]. The composition $A_4BO_{7+\delta}$ ($[A'_2O_{1+\delta}][A_2BO_6]$, i.e. $n = 2$) represents the end-member of this family with isolated BO_6 -units, while the 2H-structure can be considered the $n = \infty$ end-member. Examples for the $n = 2$ structure are $Ln_2Ca_2MnO_7$ ($Ln = La, Nd, Sm$) [7,8] and the corresponding peroxide $La_2Ca_2MnO_6(O_2)$ [9]. Our group reported on ruthenium containing samples, which were found to be rather flexible with respect to their cationic composition and can simultaneously contain oxide and

*Corresponding author. Fax: +49 821 598 3002.

E-mail address: stefan.ebbinghaus@physik.uni-augsburg.de (S.G. Ebbinghaus).

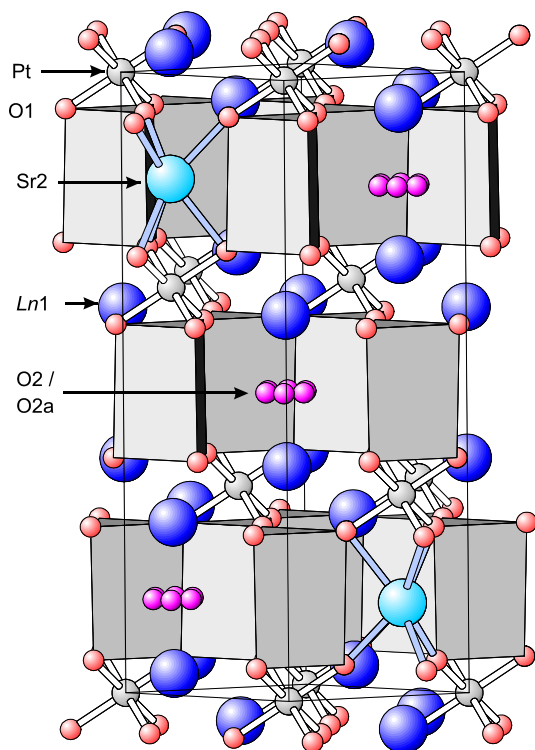


Fig. 1. Crystal structure of the $[A'_2O_{1+\delta}][A_2BO_6]$ -type hexagonal perovskites. A' cations in the trigonal prisms and A cations in the A_2BO_6 -layers are shown in light blue and dark blue, respectively. Oxygen ions in the $[A'_2O_{1+\delta}]$ -layers are colored in magenta.

peroxide ions [10–12]. The composition of these samples may be generalized as $(Ln,Sr)_{4-2z}RuO_{7-\delta}(O_2)_\delta$. The only $n=2$ compounds containing a $5d$ -transition metal are $La_{2.5}K_{1.5}IrO_7$ [13], $La_{1.2}Sr_{2.7}IrO_{6.67}(O_2)_{0.33}$ [12] and the very recently discovered platinates Ln_3NaPtO_7 ($Ln = La, Nd$) [14]. Some samples were found to exhibit interesting physical properties like high dielectric constants [15] or geometric magnetic frustration [16]. A representation of the $[A'_2O_{1+\delta}][A_2BO_6]$ structure is shown in Fig. 1.

In this paper, we describe the preparation and characterization of new $n=2$ oxides containing Pt as B -type cation. As will be shown, the three samples contain diamagnetic Pt^{4+} ions and exhibit clear indications for a symmetry reduction from space group $R\bar{3}m$ to $R\bar{3}$.

2. Experimental details

Polycrystalline samples of $Ln_2Sr_2PtO_{7+\delta}$ ($Ln = La, Pr, Nd$) were prepared by conventional solid state synthesis from $SrCO_3$, pre-dried Ln_2O_3 and Pt metal powder. Appropriate amounts of these starting materials leading to 3 g-batches were weighted with an accuracy better than 0.1 mg and thoroughly ground in an agate mortar under isopropanol. After drying, the mixtures were placed in alumina crucibles and heated for 36 h at 1100 °C in air in a box furnace.

X-ray diffraction data were collected on a Seifert XRD 3003-TT diffractometer using $CuK\alpha$ radiation in the

angular range $15^\circ \leq 2\theta \leq 150^\circ$. The step size was $0.015^\circ 2\theta$ with a counting time of 10 s per data point. For Rietveld refinement calculations the program FullProf was used [17]. The background was approximated by a linear interpolation between approximately 30 data points in regions with no Bragg reflections. The peak shape was described by a pseudo-Voigt function.

Thermogravimetric measurements were performed on a TA Q500 thermobalance. About 40 mg of the oxides were heated in flowing forming gas (10% H_2 in N_2 ; 50 ml/min) to 950 °C with a heating rate of 10 °C/min.

Optical properties of the polycrystalline powders were investigated by diffuse reflectance spectroscopy. Reflectance data were collected using a Varian Cary 500 Scan UV–Vis–NIR scanning double-beam spectrometer equipped with a 150 mm Labsphere DRA-CA-50 integrating sphere over the spectral range of 250–2000 nm (0.6–5 eV).

X-ray absorption spectroscopy at the Pt- L_{III} edge was carried out at the beamline C1 (Cemo) of the Hamburger Synchrotronstrahlungslabor (HASYLAB) at the Deutsches Elektronensynchrotron (DESY). Approximately 35 mg of each sample was mixed with polyethylene and pressed to a thin pellet of 13 mm diameter. XANES measurements were performed in transmission mode with a step width of 0.1 eV and a counting time of 2 s per data point. The energy was calibrated against the spectra of Pt metal, which was measured simultaneously.

Magnetic measurements in the temperature range $1.8 < T < 300$ K were done using a Quantum Design MPMS7 SQUID magnetometer. Samples were field-cooled (fc) in external fields of 0.1 T (Pr, Nd) and 1 T (La), respectively. The obtained values were corrected for the diamagnetic moment of the empty sample holder.

3. Results and discussion

In analogy to the previously described Ru and Ir containing samples [11,12] we first tried to prepare $La_{1.2}Sr_{2.7}PtO_{7+\delta}$. The corresponding XRD pattern clearly indicated the presence of the desired phase but also revealed a considerable amount of Sr_4PtO_6 . Further increasing the reaction time and/or temperature did not lead to significant changes in the relative peak intensities. We therefore concluded that the desired phase possesses a higher lanthanum content and in turn the oxidation state of platinum must be lower than +5. Since in the impurity phase platinum takes the oxidation state +4 it seemed reasonable to assume that this is also the case in the desired material, leading to the composition $La_2Sr_2PtO_7$. The attempt to prepare the corresponding compound resulted in a phase pure sample of yellow color. Choosing the same cationic compositions black and green samples were obtained for $Ln = Pr$ and Nd , respectively.

Rietveld refinements on the basis of X-ray diffraction were carried out starting from the structural model for $La_{1.2}Sr_{2.7}BO_{7+\delta}$ ($B = Ru, Ir$) (space group $R\bar{3}m$) described in [12]. For $Ln = Nd$ a trace impurity of Sr_4PtO_6

(≈ 1 wt%) was included in the calculations. The other two samples were single phase.

For all atoms except O2/O2a, refinement trials with anisotropic displacement parameters were carried out. The obtained ellipsoids for Ln (0, 0, 0.62) and Pt (0, 0, 0) were found to be almost spherical for all three samples. Therefore in the final runs these positions were refined with isotropic displacement parameters. For O1 the parameters β_{13} and β_{23} were fixed to 0 in order to reduce the number of variables. This simplification was based on the fact that neutron diffraction showed β_{13} and β_{23} to be close to zero for the isostructural rutenate and iridate. Furthermore, β_{33} had to be fixed to 0.0012 \AA^2 (the value obtained from neutron diffraction data of the Ru and Ir analogs) to avoid negative values in the case of Ln = Nd. These initial calculations assuming space group $R\bar{3}m$ resulted in extremely elongated displacement ellipsoids for O1. For this reason, additional refinements in the less symmetric space group $R\bar{3}$ (No. 148) were performed. The missing symmetry element (*m*) allows to shift O1 from $(x, x/2, z)$ to (x, y, z) while keeping the cationic framework unchanged. Since in $R\bar{3}$ the β_{ij} values for O1 have no restrictions, in principle six anisotropic displacement parameters need to be refined, which seems hopeless on the basis of powder X-ray diffraction. Therefore, the O1 atom was refined isotropically. In spite of the fewer free variables compared to the (anisotropic) model in $R\bar{3}m$, identical or even slightly smaller residual parameters were achieved. The estimated standard deviations (esds) for the fractional coordinates of O1 were rather small, showing that the atomic positions are well defined. In addition, the obtained B_{iso} values are in the order of $0.5\text{--}1 \text{ \AA}^2$, which is reasonable for oxygen. For these reasons we conclude that the structural model in $R\bar{3}$ is to be preferred over the one in the higher symmetric space group $R\bar{3}m$.

Attempts to refine a mixed occupation of Ln/Sr on the two *A* cation sites led to occupation factors close to 1 and 0, respectively, for Ln = Pr and Nd, indicating a complete cationic ordering. In the case of La, on the other hand, we found a significant disorder with 8.5% of the Ln^{3+} position occupied by Sr^{2+} and vice versa. The reason for this structural difference between the three compounds may result from the different sizes of the rare-earth cations. Assuming a nine-fold oxygen coordination, the ionic radii according to Shannon [18] are La^{3+} : 1.216 \AA , Pr^{3+} : 1.179 \AA , and Nd^{3+} : 1.163 \AA , while for Sr^{2+} the radius is 1.31 \AA . It therefore seems likely that only La^{3+} is large enough to allow a (partial) mixing with the strontium ions, while the other two rare earths are too small. In this context it is worth mentioning that also in $\text{La}_{1.2}\text{Sr}_{2.7}\text{BO}_{7.33}$ ($B = \text{Ru, Ir}$) a mixed La/Sr occupation was observed for the La1 site.

Earlier Rietveld refinements of $\text{La}_{1.2}\text{Sr}_{2.7}\text{BO}_{7.33}$ ($B = \text{Ru, Ir}$) gave hints for a split model with parts of the Sr2 ions located on $(0, 0, z)$ and parts on a three-fold position close to the *c*-axis. For the platinates studied in this work, on the other hand, the displacements ellipsoids of the Sr2 site were

found to be only slightly oblate and no significant remaining scattering density near the *c*-axis was detected in the difference Fourier map. It can therefore be concluded that the Sr^{2+} ions only occupy the 6*c* site and no disordered arrangement exists.

For $\text{La}_{1.2}\text{Sr}_{2.7}\text{BO}_{7.33}$ ($B = \text{Ru, Ir}$) neutron diffraction additionally revealed the oxygen atoms in the $[A'_2\text{O}_{1+\delta}]$ -layer to occupy two positions $(x, 1/2^*x, 1/2)$ and $(x, 0, 1/2)$, with different occupation and distance to the *c*-axis. Due to the small atomic form factor of oxygen, X-ray diffraction cannot resolve such structural details. For the platinates investigated here, we therefore assumed a toroidal electron density formed by equal amounts of oxygens on $(x, 1/2^*x, 1/2)$ and $(\text{Cos } 30^*x, 0, 1/2)$. For both sizes the B_{iso} was fixed to 1.0 \AA^2 .

Fig. 2 shows the Rietveld plot for $\text{La}_2\text{Sr}_2\text{PtO}_{7+\delta}$ with a magnification of the angular range $90^\circ \leq 2\theta \leq 150^\circ$ as inset. Results of the final structure refinement are listed in Tables 1 and 2. As an example Fig. 3 shows a part of the structure of $\text{Pr}_2\text{Sr}_2\text{PtO}_{7+\delta}$ with displacement parameters given at the 80% confidence level.

The cell parameters of the three title compounds are depicted in Fig. 4. As expected, both the *a* and *c* axes become shorter with decreasing ionic radius of the lanthanide ion. A comparison with the cell parameters of $\text{La}_{1.2}\text{Sr}_{2.7}\text{RuO}_{7.33}$ ($a = 5.753(1) \text{ \AA}$, $c = 18.351(3) \text{ \AA}$) and $\text{La}_{1.2}\text{Sr}_{2.7}\text{IrO}_{7.33}$ ($a = 5.771(1) \text{ \AA}$, $c = 18.348(3) \text{ \AA}$) shows that the *a* axes are of similar lengths while the *c* axes of the platinates are significantly shorter.

The lower symmetry of space group $R\bar{3}$ compared to $R\bar{3}m$ preserves the local $\bar{3}$ (D_{3d}) point symmetry of the platinum ions but strongly changes the coordination geometry of the lanthanide ions. In $R\bar{3}m$ the Ln cations within one AO_3 layer are surrounded by six equivalent O1 ions at a distance of roughly 2.9 \AA . In $R\bar{3}$, on the other hand, the six oxygens split into two sets of three ions each with bond lengths of ≈ 2.5 and $\approx 3.3 \text{ \AA}$, respectively. For Ln = La, Pr, and Nd the shorter Ln–O1 distance decreases

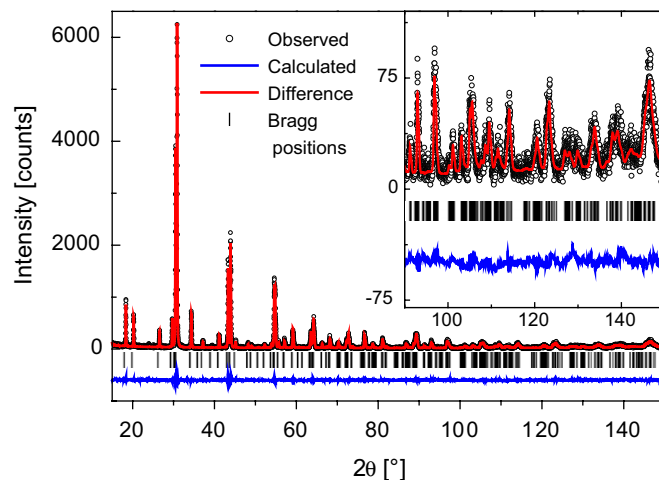


Fig. 2. XRD Rietveld refinement plot for $\text{La}_2\text{Sr}_2\text{PtO}_{7+\delta}$. The inset shows a zoom of the angular range $90^\circ \leq 2\theta \leq 150^\circ$.

Table 1
Cell parameters, atomic coordinates and (equivalent) isotropic displacement parameters for $Ln_2Sr_2PtO_{7+\delta}$

Atom	Site	a (Å) 5.7996(1) x	c (Å) 18.0750(4) y	R_p 8.68 z	R_{wp} 11.2 SOF	χ^2 1.51 $B_{iso/eq}$ (Å ²)
Pt	3a	0	0	0	1	0.74(3)
O1	18f	0.3145(15)	0.2169(18)	0.0621(4)	1	0.56(24)
La1/Sr1	6c	0	0	0.6233(1)	0.915/0.085(6)	0.99(4)
Sr2/La2 ^a	6c	0	0	0.1731(1)	0.915/0.085(6)	1.38(6) ^a
O2	18f	0.1258(52)	0	0.5	0.082(3)	1.0
O2a	18f	0.1452(62)	0.0726(31)	0.5	0.082(3)	1.0
Pr		a (Å) 5.7523(1)	c (Å) 17.8919(3)	R_p 9.26	R_{wp} 11.8	χ^2 1.34
Atom	Site	x	y	z	SOF	$B_{iso/eq}$ (Å ²)
Pt	3a	0	0	0	1	0.52(3)
O1	18f	0.3215(19)	0.2324(19)	0.0657(4)	1	0.78(28)
Pr1	6c	0	0	0.6230(1)	1	1.20(4)
Sr2 ^a	6c	0	0	0.1730(1)	1	1.61(7) ^a
O2	18f	0.1015(55)	0	0.5	0.090(3)	1.0
O2a	18f	0.1173(65)	0.0587(32)	0.5	0.090(3)	1.0
Nd		a (Å) 5.7427(1)	c (Å) 17.8770(4)	R_p 9.06	R_{wp} 11.6	χ^2 1.43
Atom	Site	x	y	z	SOF	$B_{iso/eq}$ (Å ²)
Pt	3a	0	0	0	1	0.42(3)
O1	18f	0.3237(17)	0.2370(9)	0.0641(4)	1	0.95(28)
Nd1	6c	0	0	0.6234(1)	1	0.98(4)
Sr2 ^a	6c	0	0	0.1729(1)	1	1.44(6) ^a
O2	18f	0.1218(55)	0	0.5	0.083(3)	1.0
O2a	18f	0.1407(65)	0.0703(33)	0.5	0.083(3)	1.0

Space group $R\bar{3}$ (No. 148). Parameters given without standard deviations were fixed during the refinements.

^aRefined with the anisotropic displacement parameters listed in Table 2.

Table 2
Anisotropic displacement parameters ($\exp[-(\beta_{11}h^2 + \beta_{22}k^2 + \beta_{33}l^2 + 2\beta_{12}hk + 2\beta_{13}hl + 2\beta_{23}kl)]$) for the atom Sr2

Ln	β_{11}	β_{22}	β_{33}	β_{12}	β_{13}	β_{23}
La	0.0164(11)	0.0164(11)	0.00065(9)	0.0082(5)	0	0
Pr	0.0215(12)	0.0215(12)	0.00045(10)	0.0107(6)	0	0
Nd	0.0201(11)	0.0201(11)	0.00027(9)	0.0100(6)	0	0

(2.578, 2.497, and 2.469 Å) while simultaneously the longer distance is elongated (3.265, 3.312, and 3.324 Å). In turn the coordination geometry becomes successively more irregular.

For the La and Nd containing samples the O2/O2a coordinates lead to oxygen–oxygen distances which are in reasonable agreement with the value expected for peroxide ions, while for the Pr compound the interatomic distance is significantly smaller. The site occupation factors for O2/O2a lead to total oxygen contents of 6.98(4), 7.08(4), and 7.00(4) for $Ln = La, Pr, Nd$. Within a 2σ range the Rietveld refinements therefore provide no clear proof for the presence of peroxide ions.

As a second, independent method for determining the oxygen stoichiometry thermogravimetry (TG) was used. During heating in reducing atmosphere (e.g. mixtures of H_2 with N_2 or Ar) most perovskites are reduced to the

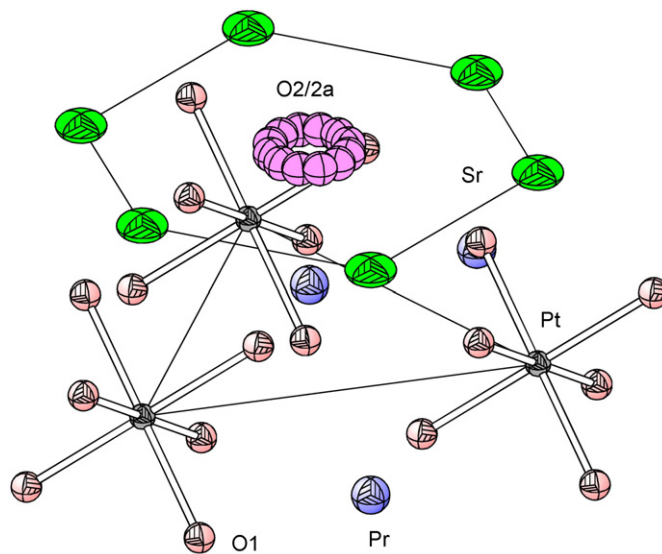


Fig. 3. Section of the crystal structure of $Pr_2Sr_2PtO_{7+\delta}$ as derived from XRD Rietveld refinement. The displacement parameters are shown with 80% probability.

corresponding metals and/or simple binary oxides, which can be identified by X-ray diffraction. From the observed weight loss and the known reaction products the oxygen content can easily be calculated. Fig. 5 gives the TG results for the three title compounds. As reduction products,

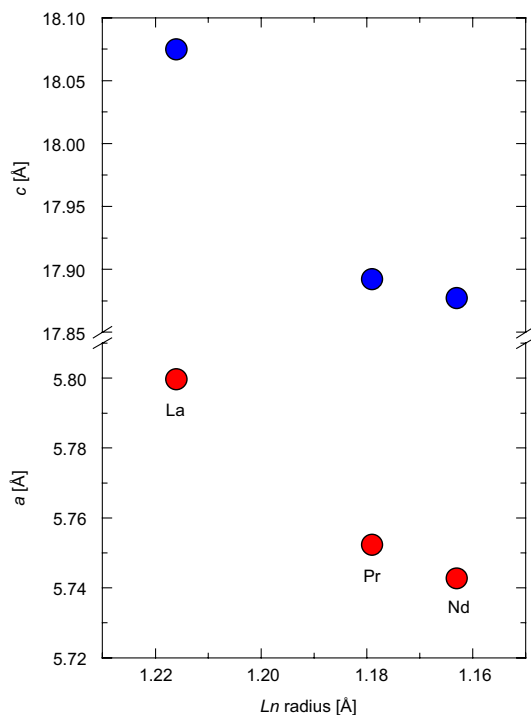


Fig. 4. Evolution of the cell parameters with changing ionic radius of the lanthanide ions. Estimated standard deviations are smaller than the size of the symbols.

Ln_2O_3 and Pt metal were identified directly after the reduction, while SrO appeared as $SrCO_3$ after keeping the reaction products in air for some days. The straight line in the figure corresponds to the expected weight loss for $\delta = 0$ in the case of $Ln = Pr$. For the other two rare earths the calculated values are very similar and therefore not shown in the figure for clarity. From Fig. 5 it is obvious that for $Ln = La$ and Pr the weight loss is larger than expected. The observed $\Delta m/m$ values of 4.46%, 4.33%, and 4.19% for La, Pr and Nd, lead to the following compositions: La $\delta = 0.13$, Pr $\delta = 0.07$, and Nd $\delta = 0.02$. The uncertainties of these values are estimated to be 0.03. Following the discussion in [11] an oxygen excess ($\delta > 0$) can be combined with the observed oxidation state of +4 of platinum (see below) by a mixed oxygen/peroxide stoichiometry according to $Ln_2Sr_2PtO_{7-\delta}(O_2)_\delta$. This means that the large hexagonal cavities in the $[A'_2O_{1+\delta}]$ -layers are occupied by both oxide (O^{2-}) and peroxide (O_2^{2-}) ions. It is noteworthy that the δ values (= peroxide contents) of the platinates studied in this work are significantly lower than those for $La_{1.2}Sr_{2.7}BO_{7+\delta}$ ($B = Ru, Ir$). For these two compounds a δ -value of 0.33 was found. In addition, in the present samples δ decreases from 0.13 to 0 going from La to Nd. The reason for this may be the shrinking of the a parameter (see Table 1), which reduces the available size for the O_2^{2-} ions in the $[A'_2O_{1+\delta}]$ -layers.

For $Ln = Pr$ and Nd the δ values obtained by thermogravimetry and XRD Rietveld refinements agree very well. In the case of $Ln = La$, on the other hand, there is a discrepancy between the TG and XRD results. While the

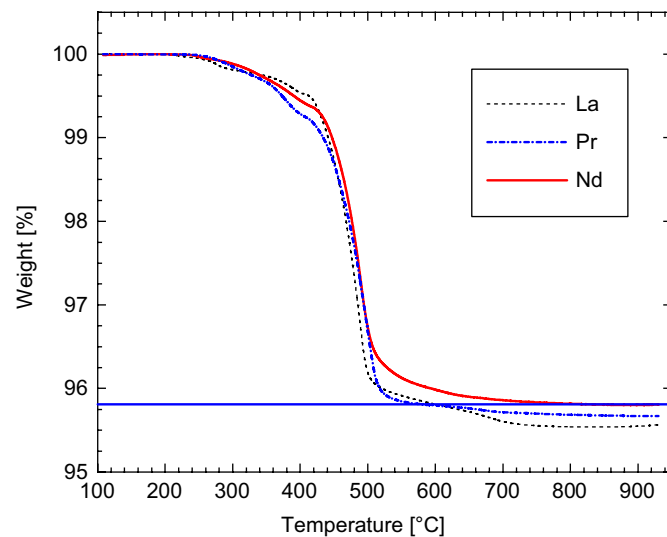


Fig. 5. Thermogravimetric investigation of the reduction of $Ln_2Sr_2PtO_{7+\delta}$. The horizontal line corresponds to the expected weight loss for $Ln = Pr$ assuming $\delta = 0$.

former method yielded an oxygen contents of 7.13, the latter resulted in a δ value close to zero. It should not be forgotten though that due to the small X-ray scattering power of oxygen, the site occupation factors for O2/O2a show rather high esd values. Furthermore, the O2/O2a occupation factor strongly correlates with the displacement parameter, which was somewhat arbitrarily fixed to 1 \AA^2 . Because of these reasons, the oxygen contents determined by thermogravimetry seem more reliable. Neutron diffraction experiments are planned for the future to verify the presence of peroxide ions in the samples.

The oxidation state of platinum was determined by X-ray absorption spectroscopy, making use of the so-called 'valence shift'. This shifting of the absorption edge to higher energies with increasing oxidation number results from a reduced shielding of the positive charge of the nucleus by the smaller number of valence electrons. In turn, the inner electrons are more tightly bound and higher energies are required for ionization. The usefulness of XANES investigations for the determination of oxidation states has been described in a series of publications for other platinum group metals like Ru and Ir [10,11,16,19–23].

Fig. 6 shows the normalized absorption spectrum of $Pr_2Sr_2PtO_{7+\delta}$ in comparison to PtO_2 , which served as Pt^{4+} -reference. As can be seen, the energetic positions of the so-called 'white lines' of these two compounds are very similar, already pointing to an oxidation state of +4 for platinum. White lines result from dipole-allowed transitions to empty orbitals with predominantly d character. Due to the crystal field splitting in an octahedral coordination, the white lines split into two sub-peaks corresponding to the t_{2g} and e_g orbitals, respectively, if the t_{2g} orbitals are only partly filled with electrons.

For a quantitative analysis, the XANES spectra were fitted according to the procedure described in [22]. For

Pt^{4+} with its $(t_{2g})^6$ configuration only one peak at the Pt- L_{III} threshold is expected, corresponding to the transition of the $2p$ electron to the empty e_g orbitals. As can be seen in Fig. 6 it was in fact possible to fit the white lines of our samples (and also of the PtO_2 reference) with only one pseudo-Voigt function for this transition and an arctangent function describing the absorption edge itself. For the energy positions of the pseudo-Voigt function the following values were obtained: $\text{La}_2\text{Sr}_2\text{PtO}_{7+\delta}$ 11.56794 keV, $\text{Pr}_2\text{Sr}_2\text{PtO}_{7+\delta}$ 11.56798 keV, and $\text{Nd}_2\text{Sr}_2\text{PtO}_{7+\delta}$ 11.56795 keV. These values agree well with the one found for PtO_2 (11.56774 keV). The deviation of roughly 0.2 eV lies well within the estimated uncertainty of the method at these energies [12]. It can therefore be concluded that platinum possesses the oxidation state +4 in $\text{Ln}_2\text{Sr}_2\text{PtO}_{7+\delta}$, as expected.

Further evidence for the oxidation state stems from magnetic measurements. For Pt^{+4} a $(t_{2g})^6$ low-spin configuration is expected. As a result $\text{La}_2\text{Sr}_2\text{PtO}_{7+\delta}$ should be diamagnetic. The SQUID measurements shown in Fig. 7 in fact reveal a small, nearly temperature-independent negative susceptibility (right scale of Fig. 7) due to the core diamagnetism of the corresponding ions. The slight upturn below 25 K may either result from the sample holder, which exhibited an increasing paramagnetic signal at these low temperatures or from traces of paramagnetic centers. For technical reasons $\text{La}_2\text{Sr}_2\text{PtO}_{7+\delta}$ was measured in an external magnetic field of 1 T, while for the other two samples a field of 0.1 T was applied. As can be seen from

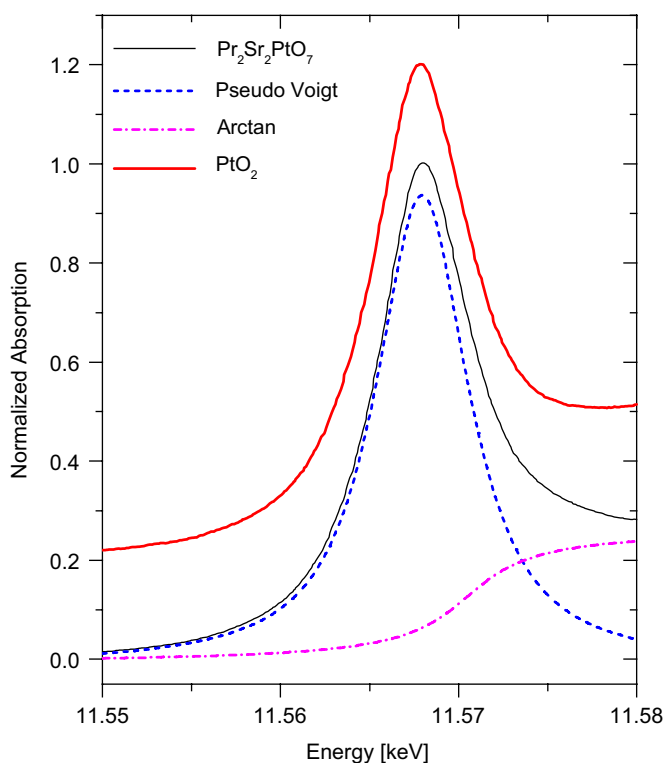


Fig. 6. Normalized XANES spectrum of $\text{Pr}_2\text{Sr}_2\text{PtO}_{7+\delta}$ in comparison to PtO_2 . The dotted lines represent the pseudo-Voigt and arctangent function used to approximate the white line and absorption edge, respectively.

Fig. 7, these two compounds exhibit almost identical strong paramagnetic signals. This similarity can be explained using the free ion approximation for the lanthanide ions. For Pr^{3+} with its $4f^2$ electronic configuration the ground term is $^3\text{H}_4$. Calculating the corresponding Landé factor yields $g = 0.8$, and the resulting magnetic moment becomes $\mu/\mu_{\text{B}} = 0.8\sqrt{20} = 3.578$. The same considerations for Nd^{3+} ($4f^3$ configuration) results in a $^4\text{I}_{9/2}$ ground term with $g = 0.7272$ and $\mu/\mu_{\text{B}} = 0.7272\sqrt{99/4} = 3.618$. The magnetic moments of these two ions are therefore expected to differ by only 1% despite of their completely different electronic configuration and ground terms.

The inset in Fig. 7 shows the experimental $1/\chi$ vs. T values for $\text{Ln} = \text{Pr}$ and Nd . The data were fitted in the temperature range 50–300 K by a modified Curie–Weiss law $\chi = (N_{\text{L}}^2\mu_0\mu^2/3R(T - T_0)) + \chi_0$ yielding the values listed in Table 3. The obtained magnetic moments per lanthanide ion are slightly smaller than the expected ones, which is not surprising taking into account that the free ion approximation neglects both crystal field effects and the contribution of higher excited states. Besides these slight discrepancies our results clearly indicate that the magnetic behavior of the two samples can be explained only by the contributions of the f -elements involved, thus confirming the presence of diamagnetic Pt^{4+} ions in $\text{Ln}_2\text{Sr}_2\text{PtO}_{7+\delta}$, as already deduced from the XANES results.

For $\text{Ln} = \text{La}$ and Nd , the samples had a yellow and green color while $\text{Pr}_2\text{Sr}_2\text{PtO}_{7+\delta}$ was black. The optical properties of $\text{La}_2\text{Sr}_2\text{PtO}_{7+\delta}$ and $\text{Nd}_2\text{Sr}_2\text{PtO}_{7+\delta}$ were investigated by measurements of their diffuse reflectance in the wavelength range 250–2000 nm. The corresponding spectra are shown in Fig. 8. While $\text{La}_2\text{Sr}_2\text{PtO}_{7+\delta}$ shows basically no absorption above approximately 500 nm, the spectrum of $\text{Nd}_2\text{Sr}_2\text{PtO}_{7+\delta}$ contains various absorption bands due to the intra-atomic f - f transitions of the Nd^{3+}

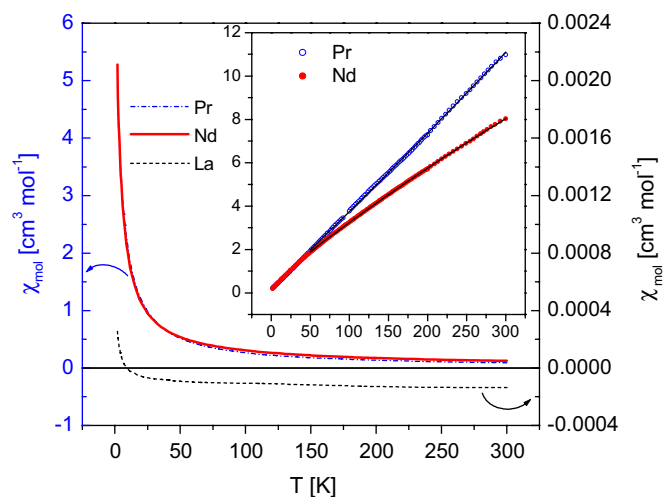


Fig. 7. Magnetic susceptibility of $\text{Ln}_2\text{Sr}_2\text{PtO}_7$. The very small diamagnetic susceptibility for $\text{Ln} = \text{La}$ is shown on the right scale. The inset shows $1/\chi$ for $\text{Ln} = \text{Pr}$ and Nd together with the fit by a Curie–Weiss behavior.

Table 3
Magnetic results obtained by Curie–Weiss fits for 50 K < T < 300 K

	μ/μ_B	T_0 (K)	χ_0 (cm ³ mol ⁻¹)
Pr ₂ Sr ₂ PtO ₇	3.040(13)	-7.1(7)	-0.0045(7)
Nd ₂ Sr ₂ PtO ₇	3.281(9)	-16.3(4)	0.0175(5)

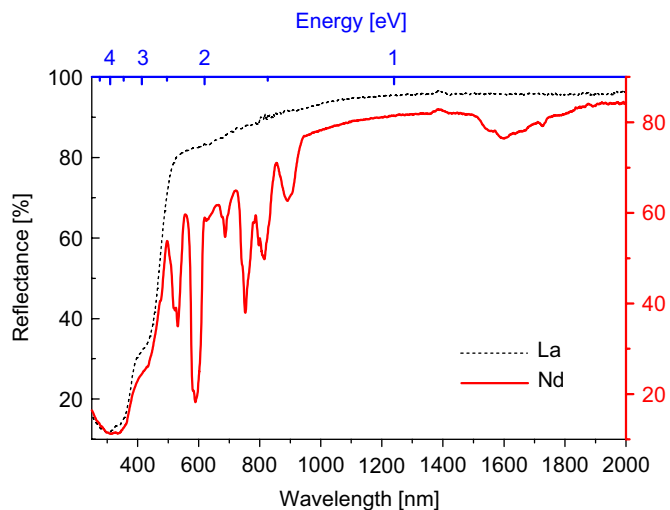


Fig. 8. UV–Vis spectra of La₂Sr₂PtO_{7+δ} and Nd₂Sr₂PtO_{7+δ}.

ions. The diffuse reflectance data were converted according to the Kubelka–Munk function $F(R) = (K/S) = (1 - R)^2 / 2R$. Band gap energies were estimated by extrapolating the onset of absorption to the wavelength axis. For both compounds the reflectance spectra show a pronounced shoulder at approximately 415 nm. Therefore, two band gap energies can be calculated. The obtained values are La₂Sr₂PtO_{7+δ}: 2.54 eV/3.07 eV; Nd₂Sr₂PtO_{7+δ}: 2.50 eV/3.03 eV. Within an estimated uncertainty of 0.05 eV the results are identical for both compounds.

The color of the samples in combination with the general catalytic activity of platinum makes these samples potentially interesting candidates for photocatalytic applications. Investigations of the photocatalytic gas phase decomposition of simple volatile organic molecules are currently carried out in our laboratory.

4. Conclusions

By conventional solid state synthesis three new compounds of the composition Ln₂Sr₂PtO_{7+δ} with Ln = La, Pr, and Nd were prepared. Besides the recently discovered Ln₃NaPtO₇ (Ln = La, Nd) these samples are the first examples for n = 2 members of the [A₂O_{1+δ}][A_nB_{n-1}O_{3n}] series of hexagonal perovskites containing platinum as B-type cation. The short list of transition metals known to form this special structural family (Mn, Nb, Ru, and Ir) was thus extended by one additional element.

The platinates reported in this work are in principle isostructural with earlier described ruthenates and iridates. Nevertheless, some remarkable structural deviations were observed. For example, we found evidences for a symmetry reduction from space group $R\bar{3}m$ to $R\bar{3}$: In the higher symmetric space group the oxygen ions forming the PtO₆-octahedra (O1, positioned at roughly (0.32, 0.16, 0.06)) exhibited extremely elongated displacement ellipsoids while in $R\bar{3}$ the refinements indicated a shift of these ions to approximately (0.32, 0.22, 0.06). In addition, a complete ordering of Ln³⁺ and Sr²⁺ on the two distinct crystallographic A-sites was found for Pr and Nd, while for La a slightly disordered arrangement was observed. Furthermore, no indications for vacancies on the Sr2 sites could be found and the Sr²⁺ ions occupy only the 6c site (0, 0, z), in contrast to La_{1.2}Sr_{2.7}BO_{7+δ} (B = Ru, Ir) where a fraction of Sr²⁺ ions takes a (2x, x, z) position. Finally, the δ values are significantly lower than in the corresponding Ru- and Ir-based compounds, indicating a much smaller content of peroxide ions, which decreases from 0.13 to zero for Ln = La and Nd.

Magnetic measurements proved La₂Sr₂PtO_{7+δ} to be diamagnetic in accordance with the expected low-spin (*t*_{2g})⁶ electronic configuration of Pt⁴⁺. For Ln = Pr and Nd the observed paramagnetism can well be explained by the magnetic moment of the respective rare-earth ions.

The oxidation state of platinum was additionally investigated using X-ray absorption spectroscopy. By comparing the energy position of the white line at the Pt-L_{III} absorption edge with the PtO₂ reference, platinum was found to be tetravalent in all three samples, in accordance with the magnetic measurements. UV–Vis diffuse reflectance data were recorded for the yellow La and green Nd samples. Both compounds yielded optical band gaps of roughly 3.05 eV with an additional transition at 2.5 eV.

As described above, a good structural model in space group $R\bar{3}$ was obtained. Nevertheless, X-ray diffraction does not allow an unambiguous determination of the correct space group. Also the site occupation of the O2/O2a position and in turn the total oxygen content cannot be determined with the desired accuracy. These questions will be addressed in the near future using neutron diffraction.

Acknowledgments

Thanks are due to HASYLAB for allocating synchrotron beamtime. This work was supported by the Deutsche Forschungsgemeinschaft (DFG) through SFB 484.

References

- [1] L.J. Bie, Y.X. Wang, J.H. Lin, C.K. Loong, J.W. Richardson, L.P. You, C. Dong, Chem. Mater. 15 (2003) 516.
- [2] L. Bie, J. Lin, Y. Wang, C.-K. Loong, Inorg. Chem. Commun. 5 (2002) 966.

- [3] F. Grasset, M. Zakhour, J. Darriet, J. Alloys Compd. 287 (1999) 25.
- [4] C. Dussarrat, J. Fompeyrine, J. Darriet, Eur. J. Solid State Inorg. Chem. 31 (1994) 289.
- [5] F. Grasset, C. Dussarrat, J. Darriet, J. Mater. Chem. 7 (1997) 1911.
- [6] S.J. Kim, M.D. Smith, J. Darriet, H.-C. zur Loye, J. Solid State Chem. 177 (2004) 1493.
- [7] Y. Wang, J. Lin, Y. Du, R. Qin, B. Han, C.K. Loong, Angew. Chem. Int. Ed. 39 (2000) 2730.
- [8] Y. Wang, L. Bie, Y. Du, J. Lin, C.-K. Loong, J. Richardson, L. You, J. Solid State Chem. 177 (2004) 65.
- [9] E. Gaudin, G. Goglio, A. Besnard, J. Darriet, J. Solid State Chem. 175 (2003) 124.
- [10] S.G. Ebbinghaus, J. Solid State Chem. 177 (2004) 817.
- [11] T. Götzfried, A. Reller, S.G. Ebbinghaus, Solid State Sci. 6 (2004) 1205.
- [12] T. Götzfried, A. Reller, S.G. Ebbinghaus, Inorg. Chem. 44 (2005) 6550.
- [13] S.J. Mugavero III, M.D. Smith, H.-C. zur Loye, J. Solid State Chem. 178 (2005) 3176.
- [14] T.J. Hansen, R.B. Macquart, M.D. Smith, H.-C. zur Loye, Solid State Sci. 9 (2007) 785.
- [15] P. Lunkenheimer, T. Götzfried, R. Fichtl, S. Weber, T. Rudolf, A. Loidl, A. Reller, S.G. Ebbinghaus, J. Solid State Chem. 179 (2006) 3965.
- [16] S.G. Ebbinghaus, E.-W. Scheidt, T. Götzfried, Phys. Rev. B 75 (2007) 144414.
- [17] J. Rodríguez-Carvajal, Abstracts of the Satellite Meeting on Powder Diffraction of the XV Congress of the IUCr, 1990, p. 127.
- [18] R.D. Shannon, Acta Crystallogr. A 32 (1976) 751.
- [19] J.-H. Choy, J.-Y. Kim, S.-H. Hwang, S.-J. Kim, G. Demazeau, Int. J. Inorg. Mater. 2 (2000) 61.
- [20] J.-H. Choy, D.-K. Kim, G. Demazeau, D.-Y. Jung, J. Phys. Chem. 98 (1994) 6258.
- [21] J.-H. Choy, D.-K. Kim, S.-H. Hwang, G. Demazeau, D.-Y. Jung, J. Am. Chem. Soc. 117 (1995) 8557.
- [22] S. Ebbinghaus, Z. Hu, A. Reller, J. Solid State Chem. 156 (2001) 194.
- [23] Z. Hu, H. von Lips, M.S. Golden, J. Fink, G. Kaindl, F.M.F. de Groot, S. Ebbinghaus, A. Reller, Phys. Rev. B 61 (2000) 5262.